Translational Oncology
www.transonc.com

Volume 10 Number 2 April 2017 pp. 158–167 158

The Effect of Sunitinib Treatment in Human Melanoma Xenografts: Associations with Angiogenic Profiles[1]

Jon-Vidar Gaustad, Trude G. Simonsen, Lise Mari K. Andersen and Einar K. Rofstad

Group of Radiation Biology and Tumor Physiology, Department of Radiation Biology, Institute for Cancer Research, Oslo University Hospital, Oslo, Norway

Abstract

The effect of antiangiogenic agents targeting the vascular endothelial growth factor A (VEGF-A) pathway has been reported to vary substantially in preclinical studies. The purpose of this study was to investigate the effect of sunitinib treatment on tumor vasculature and oxygenation in melanoma xenografts with different angiogenic profiles. A-07, U-25, D-12, or R-18 melanoma xenografts were grown in dorsal window chambers and given daily treatments of sunitinib (40 mg/kg) or vehicle. Morphologic parameters of tumor vascular networks were assessed from high-resolution transillumination images, and tumor blood supply times (BSTs) were assessed from first-pass imaging movies. Tumor hypoxia was assessed with immunohistochemistry by using pimonidazole as hypoxia marker, and the gene expression and the protein secretion rate of angiogenic factors were assessed by quantitative polymerase chain reaction and enzyme-linked immunosorbent assay, respectively. The melanoma lines differed substantially in the expression of VEGF-A, VEGF-C, and platelet-derived growth factor A. Sunitinib treatment reduced vessel densities and induced hypoxia in all melanoma lines, and the magnitude of the effect was associated with the gene expression and protein secretion rate of VEGF-A. Sunitinib treatment also increased vessel segment lengths, reduced the number of small-diameter vessels, and inhibited growth-induced increases in the diameter of surviving vessels but did not change BST. In conclusion, sunitinib treatment did not improve vascular function but reduced vessel density and induced hypoxia in human melanoma xenografts. The magnitude of the treatment-induced effect was associated with the VEGF-A expression of the melanoma lines.

Translational Oncology (2017) 10, 158–167

Introduction

Solid tumors need to develop vasculature that can supply the tumor cells with oxygen and nutrients to grow beyond a few millimeters in size [1]. Tumor cells secrete several proteins that stimulate or inhibit angiogenesis, and the rate of angiogenesis is given by the ratio between these pro- and antiangiogenic factors [2]. Several strategies have been developed to inhibit angiogenesis. These include monoclonal antibodies that target proangiogenic factors or their receptors [3,4], tyrosine kinase inhibitors that may inhibit multiple receptors [5], and endogenous or exogeneous antiangiogenic factors [6].

There is substantial evidence that melanoma progression requires induction of angiogenesis. Thus, the transition from the radial to the vertical growth phase, which represents a worsening of prognosis, has been shown to be dependent on neovascularization [7]. Moreover, the probability of metastasis has been found to increase with increasing microvessel density in the primary tumor [8]. Despite this, antiangiogenic treatments have failed to prolong survival for patients with malignant melanoma, and no antiangiogenic drug has been approved for this group [9]. Currently, the effect of antiangiogenic treatments in combination with conventional chemotherapy or immunotherapy is investigated for patients with malignant melanoma [9].

Address all correspondence to: Jon-Vidar Gaustad, Group of Radiation Biology and Tumor Physiology, Department of Radiation Biology, Institute for Cancer Research, Oslo University Hospital, Montebello, N-0310, Oslo, Norway.
E-mail: Jon.Vidar.Gaustad@rr-research.no

[1] Financial support was received from the Norwegian Cancer Society and the South-Eastern Norway Regional Health Authority. The funding sources had no role in study design; in the collection, analysis, and interpretation of data; in the writing of the report; and in the decision to submit the article for publication.
Received 3 November 2016; Revised 7 December 2016; Accepted 16 December 2016

1936-5233/17
http://dx.doi.org/10.1016/j.tranon.2016.12.007

The effect of conventional chemotherapy and immunotherapy can be substantially affected by the tumor microenvironment. Hypoxic tumors are more resistant to immunotherapy, and some form of chemotherapy and poor blood supply can impair the uptake of therapeutic drugs [10,11]. Antiangiogenic treatments have been shown to improve blood supply and oxygenation in some preclinical studies [3,4] and to induce hypoxia in others [12,13]. The reasons for these apparently opposite effects on the tumor microenvironment are not well understood but may have substantial impact on combination therapy [14]. It has been suggested that antiangiogenic treatment only improves blood supply and oxygenation for a short time period and that this time period may differ for different tumor models [4]. However, it has also been suggested that this beneficial effect does not occur in all tumor models [12].

Sunitinib is a tyrosine kinase inhibitor which targets several receptors including vascular endothelial growth factor receptors 1 to 3 (VEGFR-1, -2, and -3) and platelet-derived growth factor receptors α and β (PDGFR-α and PDGFR-β) [5]. Sunitinib has been shown to prolong survival for patients with imatinib-refractory gastrointestinal stromal tumor; metastatic renal cell carcinoma; and progressive, well-differentiated pancreatic neuroendocrine tumor and has been approved by the US Food and Drug Administration for these indications [15–17]. We are currently investigating the effect of sunitinib treatment in preclinical models of malignant melanoma in our laboratory [18,19]. In the current study, we investigated the effect of sunitinib treatment in four melanoma models and measured the expression and secretion rate of several angiogenic factors in the models. The tumors were grown in dorsal window chambers in mice, and the tumor vasculature was evaluated multiple times during treatment by applying intravital microscopy techniques. We show that sunitinib treatment reduced vessel density and induced hypoxia in all melanoma models and that the magnitude of the effect was associated with the expression and secretion rate of VEGF-A.

Materials and Methods

Tumor Model

A-07, U-25, D-12, and R-18 human melanoma cells transfected with green fluorescence protein (GFP) obtained from our frozen stock were used in the present experiments [20]. Window chambers were surgically implanted in the dorsal skin fold of adult female BALB/c *nu/nu* mice, and tumors were initiated by implanting multicellular spheroids or tumor specimens with a diameter of 200 to 400 μm as reported earlier [21]. The animal experiments were approved by the Norwegian National Animal Research Authority and were done according to the Interdisciplinary Principles and Guidelines for the Use of Animals in Research, Marketing, and Education (New York Academy of Sciences, New York, NY).

Anesthesia

Window chamber implantation and intravital microscopy examinations were carried out with anesthetized mice. Fentanyl citrate (Janssen Pharmaceutica, Beerse, Belgium), fluanisone (Janssen Pharmaceutica), and midazolam (Hoffmann-La Roche, Basel, Switzerland) were administered intraperitoneally in doses of 0.63 mg/kg, 20 mg/kg, and 10 mg/kg, respectively.

Sunitinib Treatment

Sunitinib L-malate (LC Laboratories, Woburn, MA) was dissolved in hydrochloric acid (1.0 molar ratio of sunitinib), polysorbate 80 (0.5%; Sigma-Aldrich, Schnelldorf, Germany), polyethylene glycol 300 (10%; Sigma-Aldrich), sodium hydroxide (to adjust pH to 3.5), and sterile water. Mice were treated with 40 mg/kg/day sunitinib or vehicle for 4 days by oral administration.

Intravital Microscopy

Mice with window chambers were fixed to the microscope stage during intravital microscopy, and the body core temperature was kept at 37°C to 38°C by using a hot-air generator. Imaging was performed by using an inverted fluorescence microscope (IX-71; Olympus, Munich, Germany) and a black and white CCD camera (C9300-024; Hamamatsu Photonics, Hamamatsu, Japan). Tumor vasculature was visualized by using a ×4 objective lens, transillumination, and filters for green light, resulting in images with a pixel size of 3.7 × 3.7 μm^2. To study the function of tumor vasculature, first-pass imaging movies were recorded after a 0.2-ml bolus of 50 mg/ml of tetramethylrhodamine isothiocyanate–labeled dextran (Sigma-Aldrich) with a molecular weight of 155 kDa was injected into the lateral tail vein. First-pass imaging movies were recorded at a frame rate of 22.3 frames per second by using a ×2 objective lens, resulting in a time resolution of 44.8 milliseconds and a pixel size of 7.5 × 7.5 μm^2.

Image Processing

Vessel density (i.e., total vessel length per mm^2 tumor area), interstitial distance (i.e., the distance from a tumor pixel outside the vascular mask to the nearest pixel within the vascular mask), and median vessel diameter were computed from manually produced vascular masks by applying algorithms implemented in MATLAB software (The MathWorks, Natick, MA), as previously described [21]. Vessel segment length (i.e., the distance between the branching points along the vessel) was calculated from ~50 randomly selected vessel segments. Change in vessel diameter was assessed by manually measuring the diameter of the same vessel segments on subsequent days. Blood supply time (BST) images were produced by assigning a BST value to each pixel of the vascular masks [21]. The BST of a pixel was defined as the time difference between the frame showing maximum fluorescence intensity in the pixel and the frame showing maximum fluorescence intensity in the main tumor supplying artery, as described in detail previously [22]. Tumor size (i.e., tumor area) was calculated from the number of pixels showing GFP fluorescence.

Immunohistochemical Detection of Tumor Hypoxia and Pericytes

The tumors were resected immediately after the last intravital microscopy examinations and fixed in phosphate-buffered 4% paraformaldehyde. Pimonidazole [1-[(2-hydroxy-3-piperidinyl)-propyl]-2-nitroimidazole] was administered as described previously and used as hypoxia marker [23], and α-smooth muscle actin (α-SMA) was used as marker for pericytes. Immunohistochemistry was done by using a peroxidase-based indirect staining method [23]. An antipimonidazole rabbit polyclonal antibody (gift from Prof. J.A. Raleigh, Department of Radiation Oncology, University of North Carolina School of Medicine, Chapel Hill, NC) or an anti–α-SMA rabbit polyclonal antibody (Abcam, Cambridge, United Kingdom) was used as primary antibody, diaminobenzidine was used as chromogen, and hematoxylin was used for counterstaining. Hypoxic area fractions were determined by image analysis.

Quantitative Polymerase Chain Reaction (PCR)

RNA isolation, cDNA synthesis, and quantitative PCR were performed as described in detail previously for cells in culture [24]. Briefly, gene expression was assessed by using the RT^2 Profiler PCR

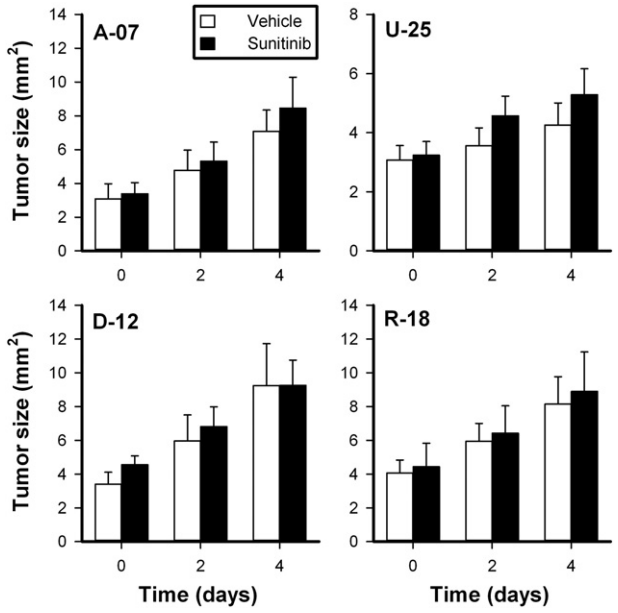

Figure 1. Untreated and sunitinib-treated tumors did not differ in tumor size. Tumor size versus time for untreated and sunitinib-treated A-07, U-25, D-12, and R-18 tumors. Columns, means of six to nine tumors; bars, SEM. Significant differences in tumor size between untreated and sunitinib-treated tumors were not found ($P > .05$).

Array Human Angiogenesis (PAHS-024A) from SABiosciences (Frederick, MD). Real-time PCR was performed on an ABI 7900HT Fast Real-Time PCR instrument (Applied Biosystems, Carlsbad, CA). Each tumor line was run in three biological replicates. Glyceraldehyde-3-phosphate dehydrogenase (GAPDH) and β-actin (ACTB) were used as normalization genes because these housekeeping genes showed stable expression across the melanoma lines studied here. Thus, each replicate C_T value was normalized to the mean C_T value of GAPDH and ACTB ($\Delta C_T = C_T^{\text{gene of interest}} - C_T^{\text{mean of GADPH and ACTB}}$).

Enzyme-Linked Immunosorbent Assay (ELISA)

Medium samples from cell cultures in exponential growth were collected 24 hours after change of medium. Commercial ELISA kits (Quantikine; R&D Systems, Abingdon, United Kingdom) were used according to the manufacturer's instructions to measure the concentration of VEGF-A in the medium samples as described previously [25].

Statistical Analysis

Statistical comparisons of data were carried out by the Student's *t* test when the data complied with the conditions of normality and equal variance. Under other conditions, comparisons were done by nonparametric analysis using the Mann-Whitney rank sum test. Probability values of $P < .05$, determined from two-sided tests, were considered significant. The statistical analysis was performed by using the SigmaStat statistical software (SPSS Science, Chicago, IL).

Results

Mice with tumors of similar size were given sunitinib treatment or vehicle after the tumors had developed vascular networks. The tumors were subjected to intravital microscopy before the treatment started (day 0) and twice during the treatment period (day 2 and 4), allowing accurate measurement of tumor size at these time points. The sunitinib-treated tumors did not differ from the untreated tumors in size at any time point ($P > .05$; Figure 1), implying that any difference between the tumor groups was not caused by differences in tumor size.

Figure 2 shows intravital microscopy images of the vasculature and an immunohistochemical preparation of the imaged tissue stained for

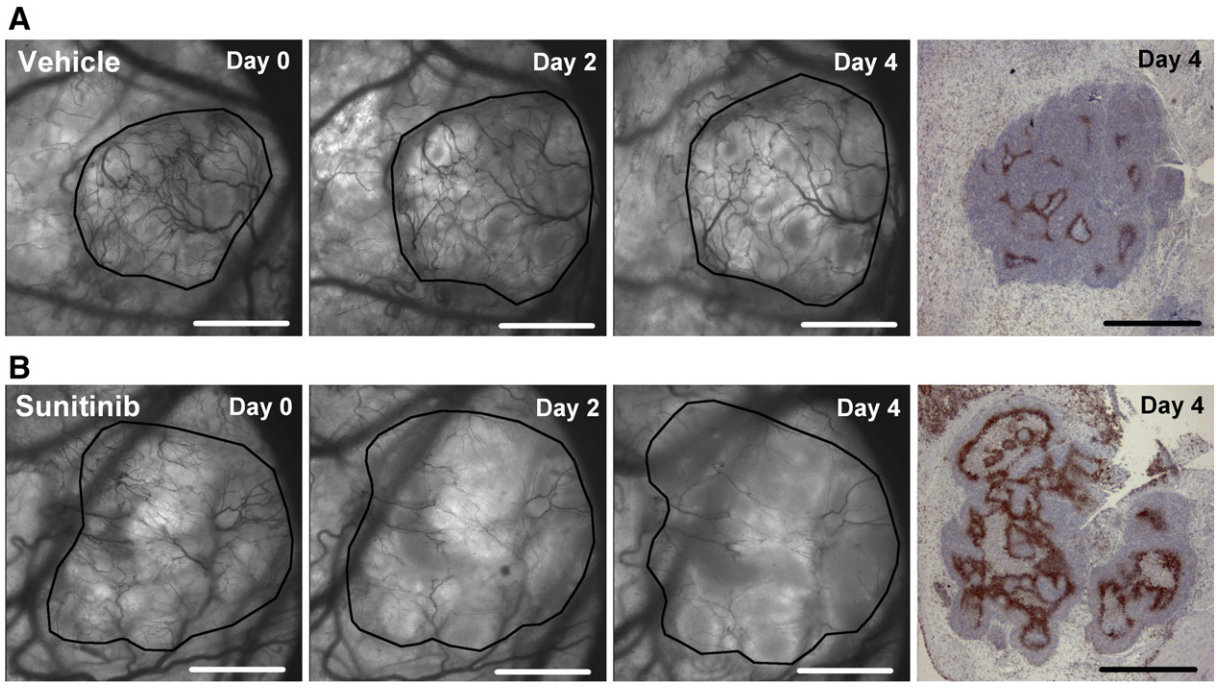

Figure 2. Images of tumor vascular networks and hypoxia. Intravital microscopy images recorded before (day 0) and during treatment (days 2 and 4), and immunohistochemical preparations of the imaged tissue stained for pimonidazole to visualize hypoxia (day 4). The images show a representative untreated U-25 tumor (A) and a representative sunitinib-treated U-25 tumor (B). Tumor area is delineated by a solid black line in intravital microscopy images. Scale bars, 1 mm.

hypoxia. The images show a representative untreated U-25 tumor (Figure 2*A*) and a representative sunitinib-treated U-25 tumor (Figure 2*B*). Similar images of representative A-07, D-12, and R-18 tumors are shown in Supplementary Figure S1. These images illustrate that sunitinib treatment decreased vessel densities and induced hypoxia, and that hypoxic regions colocalized with regions with low vascular density. Quantitative studies confirmed that sunitinib-treated tumors showed significantly lower vessel densities and significantly higher interstitial distances than untreated tumors ($P < .05$; Figure 3, *A* and *B*). The sunitinib-induced decrease in

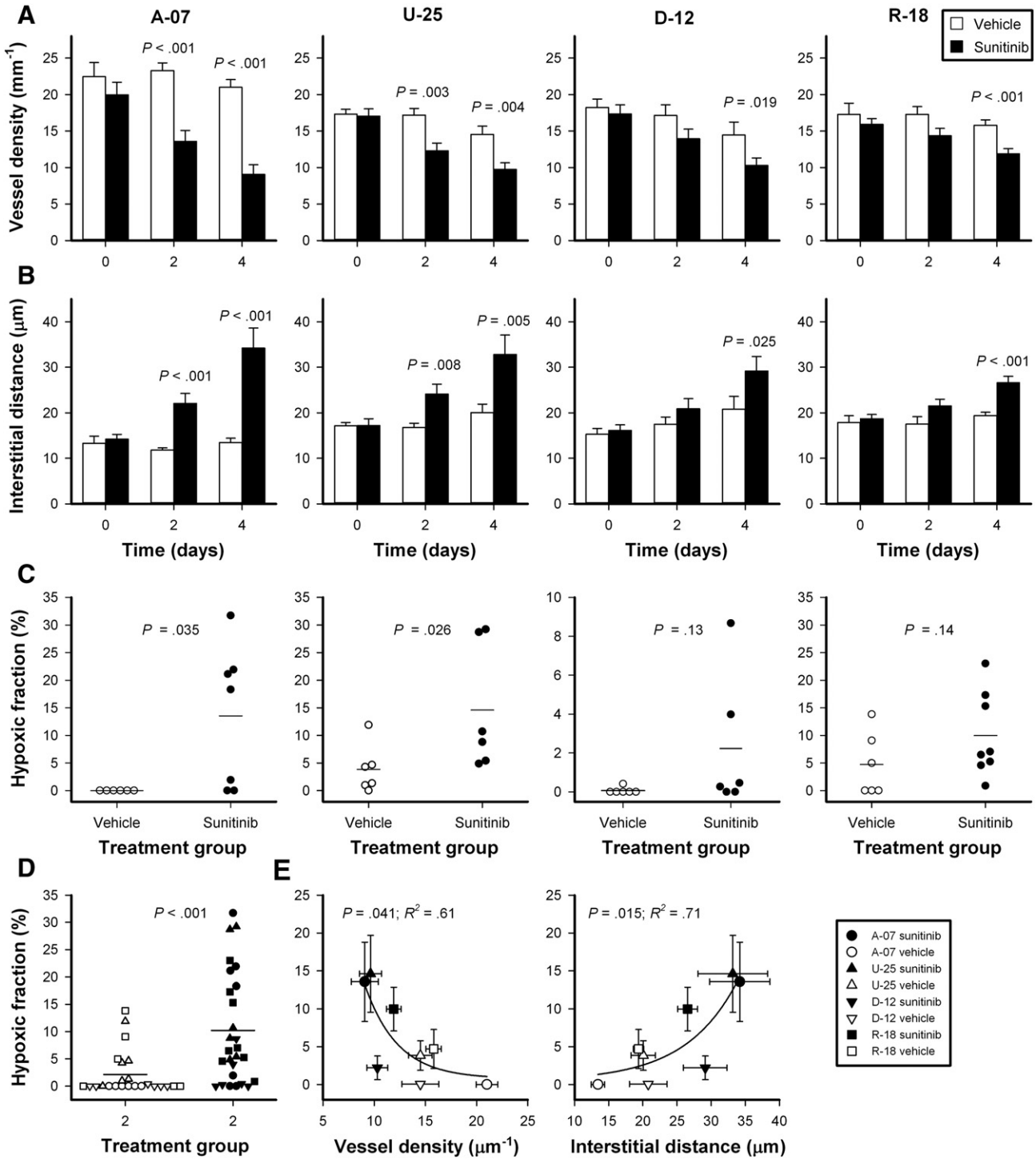

Figure 3. Sunitinib treatment reduced vessel density and induced hypoxia. (A–D) Vessel density versus time (A), interstitial distance versus time (B), and hypoxic fraction (C and D) in untreated and sunitinib-treated A-07, U-25, D-12, and R-18 tumors. Columns, means of six to nine tumors (A and B); bars, SEM (A and B); points, individual tumors (C and D). Individual tumors from each tumor lines are shown in separate panels (C) and pooled together (D). *P* values are indicated in the panels where statistical tests revealed significant or borderline significant differences between untreated and sunitinib-treated tumors. (E) Hypoxic fraction versus vessel density and hypoxic fraction versus interstitial distance for untreated and sunitinib-treated A-07, U-25, D-12, and R-18 tumors. Points, means of six to nine tumors; bars, SEM; lines, curves fitted to the data by regression analysis. R^2 and *P* value determined from regression analysis are indicated in the panels.

vessel density was 53% for A-07 tumors, 26% for U-25 tumors, 19% for D-12 tumors, and 17% for R-18 tumors. Sunitinib-treated tumors showed higher hypoxic fractions than untreated tumors. This difference was significant for A-07 and U-25 tumors ($P = .035$ and $P = .026$, respectively; Figure 3*C*), borderline significant for D-12 and R-18 tumors ($P = .13$ and $P = .14$, respectively; Figure 3*C*), and highly significant when A-07, U-25, D-12, and R-18 tumors were pooled together ($P < .001$; Figure 3*D*). Moreover, significant correlations were found between hypoxic fraction and vessel density ($P = .041$, $R^2 = .61$; Figure 3*E*) and between hypoxic fraction and interstitial distance ($P = .015$, $R^2 = .71$; Figure 3*E*).

Sunitinib treatment also affected individual vessels. Sunitinib-treated tumors showed significantly longer vessel segments than untreated tumors ($P < .05$; Figure 4*A*), and there was a trend towards increased

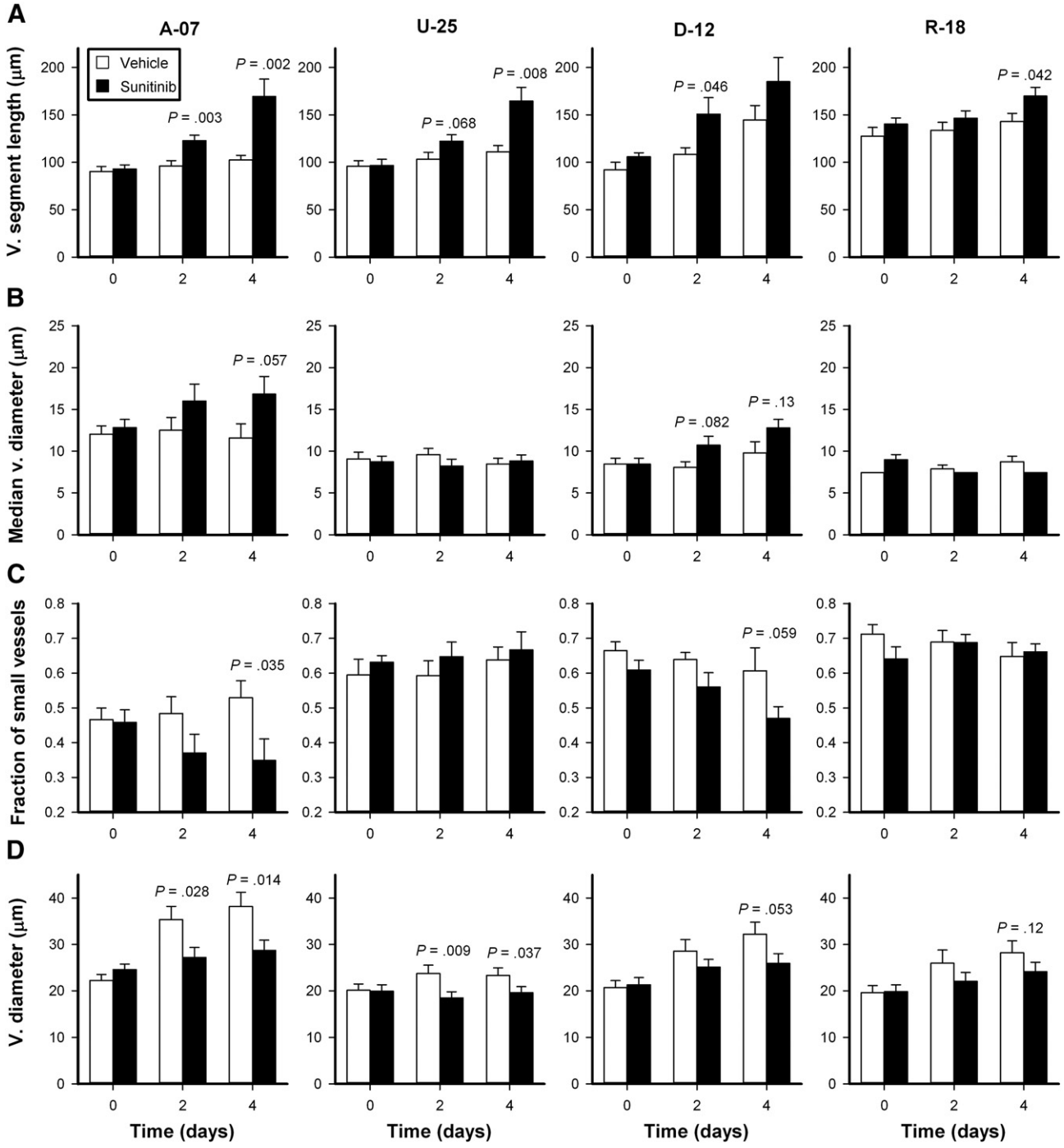

Figure 4. The effect of sunitinib treatment on individual vessels. Vessel segment length (A), median vessel diameter (B), fraction of small vessels (C), and vessel diameter (D) versus time for untreated and sunitinib-treated A-07, U-25, D-12, and R-18 tumors. Median vessel diameter was calculated by including all vessels in the tumor vascular network (B). In addition, the same individual vessels were identified on subsequent days, and the diameters of these were measured (D). These measurements show how the diameter changed in surviving vessels. The fraction of small vessels refers to the fraction of vessels with diameter < 5 μm (C). Columns, means of six to nine tumors; bars, SEM. *P* values are indicated in the panels where statistical tests revealed significant or borderline significant differences between untreated and sunitinib-treated tumors.

median vessel diameter in sunitinib-treated A-07 and D-12 tumors ($P = .057$ and $P = .13$, respectively; Figure 4*B*). Both selective removal of small-diameter vessels and increases in the diameter of remaining vessels may result in increased median vessel diameter. The fraction of small-diameter vessels was reduced in sunitinib-treated A-07 and D-12 tumors but was not changed in sunitinib-treated U-25 and R-18 tumors (Figure 4*C*). In untreated tumors, the diameter of individual vessels increased during growth, whereas growth-induced increases in vessel diameter were reduced or inhibited in sunitinib-treated tumors (Figure 4*D*). Taken together, these observations suggest that sunitinib treatment selectively removed small-diameter vessels in A-07 and D-12 tumors and reduced growth-induced diameter increases in the surviving vessels in all tumor lines.

To investigate sunitinib-induced effects on vascular function, first-pass imaging movies were recorded, and BST images and BST frequency distributions were produced. A first-pass imaging movie of a representative untreated U-25 tumor is shown in Supplementary Movie 1. Figure 5, *A* and *B*, shows BST images and the corresponding BST frequency distributions of a representative untreated U-25 tumor (Figure 5*A*) and a representative sunitinib-treated U-25 tumor (Figure 5*B*). Similar images and frequency distributions of representative A-07, D-12, and R-18 tumors are presented in Supplementary Figure S2. Sunitinib-treated tumors did not differ from untreated tumors in BST on either day 2 or day 4 ($P > .05$; Figure 5*C*).

Histological preparations of the tumors were stained with α-SMA to visualize pericytes. Sunitinib-treated tumors did not differ from untreated tumors in pericyte coverage. This is illustrated in Figure 6, which shows that both small- and large-diameter vessels were covered with pericytes in A-07 tumors. The melanoma models generally showed low levels of infiltrating immune cells, and these levels were not increased in sunitinib-treated tumors. Differences in cell density between untreated and sunitinib-treated tumors were not found.

The VEGF-A gene expression and secretion rates were significantly higher in the A-07 line than in the U-25, D-12, and R-18 line and significantly higher in the U-25 line than in the D-12 and R-18 line ($P < .05$; Figure 7, *A* and *B*). The VEGF-C gene expression was significantly higher in the A-07 line than in the U-25, D-12, and R-18 line and significantly higher in the D-12 line than in the U-25 and R-18 line ($P < .05$; Figure 7*C*). The PDGFA gene expression was significantly higher in the D-12 line than in the A-07, U-25, and

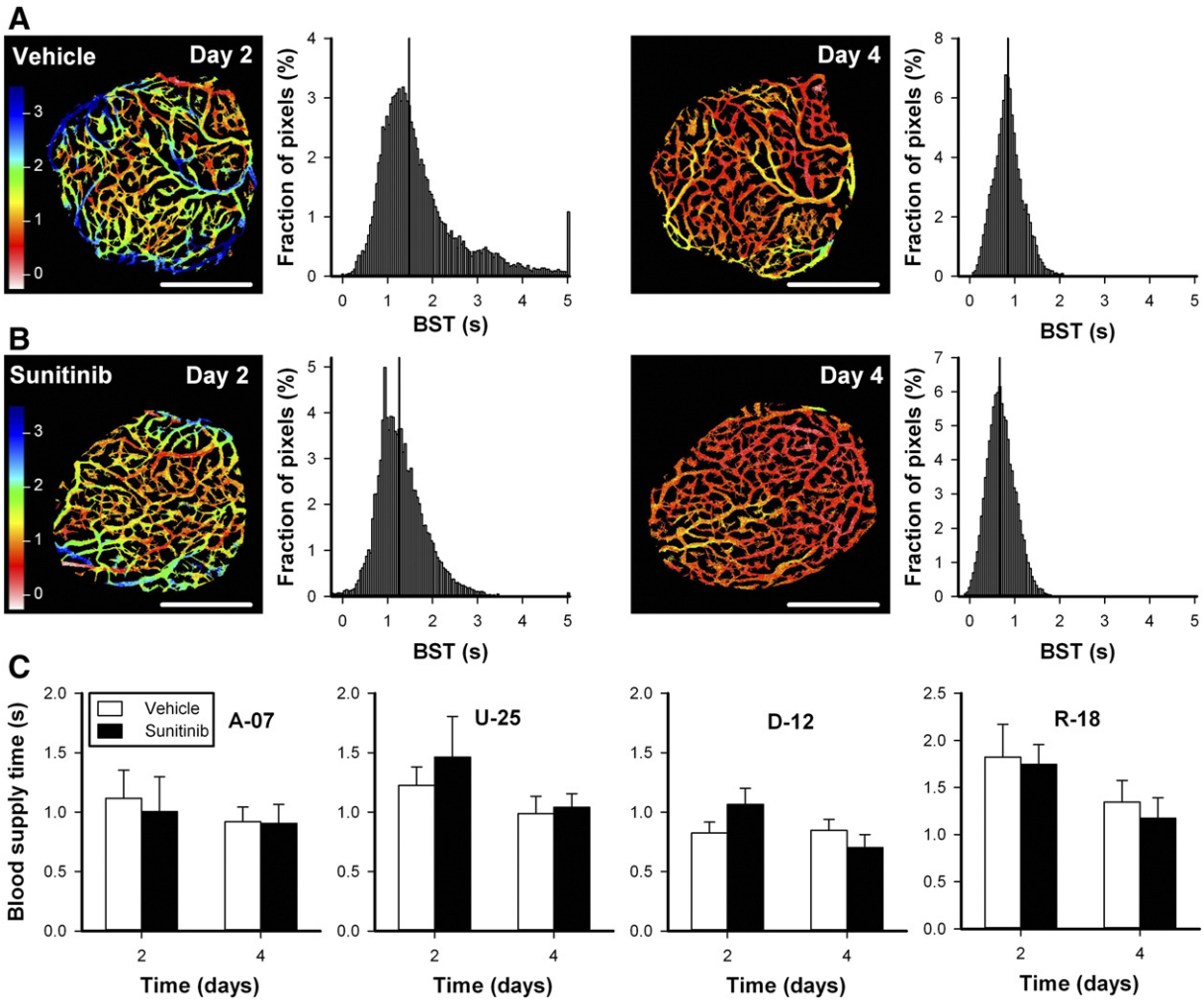

Figure 5. Sunitinib treatment did not affect BST. (A and B) BST images and the corresponding BST frequency distributions from days 2 and 4 of a representative untreated U-25 tumor (A) and a representative sunitinib-treated U-25 tumor (B). Color bars, BST scale in seconds; scale bars, 1 mm; vertical lines, median BST. (C) BST versus time for untreated and sunitinib-treated A-07, U-25, D-12, and R-18 tumors. Columns, mean of five to nine tumors; bars, SEM. Significant differences in BST between untreated and sunitinib-treated tumors were not found ($P > .05$).

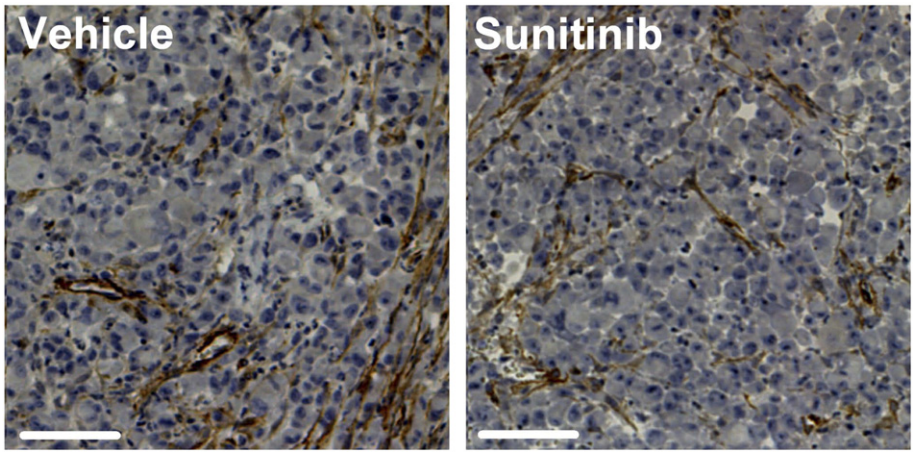

Figure 6. Immunohistochemical detection of pericytes. Immunohistochemical preparations stained with anti–α-SMA antibody of a representative untreated A-07 tumor (left) and a representative sunitinib-treated A-07 tumor (right). Scale bars, 100 μm.

R-18 line ($P < .05$; Figure 7*D*). The decrease in vessel density after 4 days of sunitinib treatment was calculated from Figure 3*A*. Significant correlations were found between the sunitinib-induced decrease in vessel density and VEGF-A gene expression and secretion rate (vessel density decrease versus VEGF-A gene expression: $P = .023$, $R^2 = .96$, Figure 7*E*; vessel density decrease versus VEGF-A secretion rate: $P = .011$, $R^2 = .99$, Figure 7*F*). A-07 tumors showed the largest decrease in vessel density and the highest VEGF-C gene expression; however, when all tumor lines were considered, significant correlations between the sunitinib-induced decrease in vessel density and VEGF-C gene

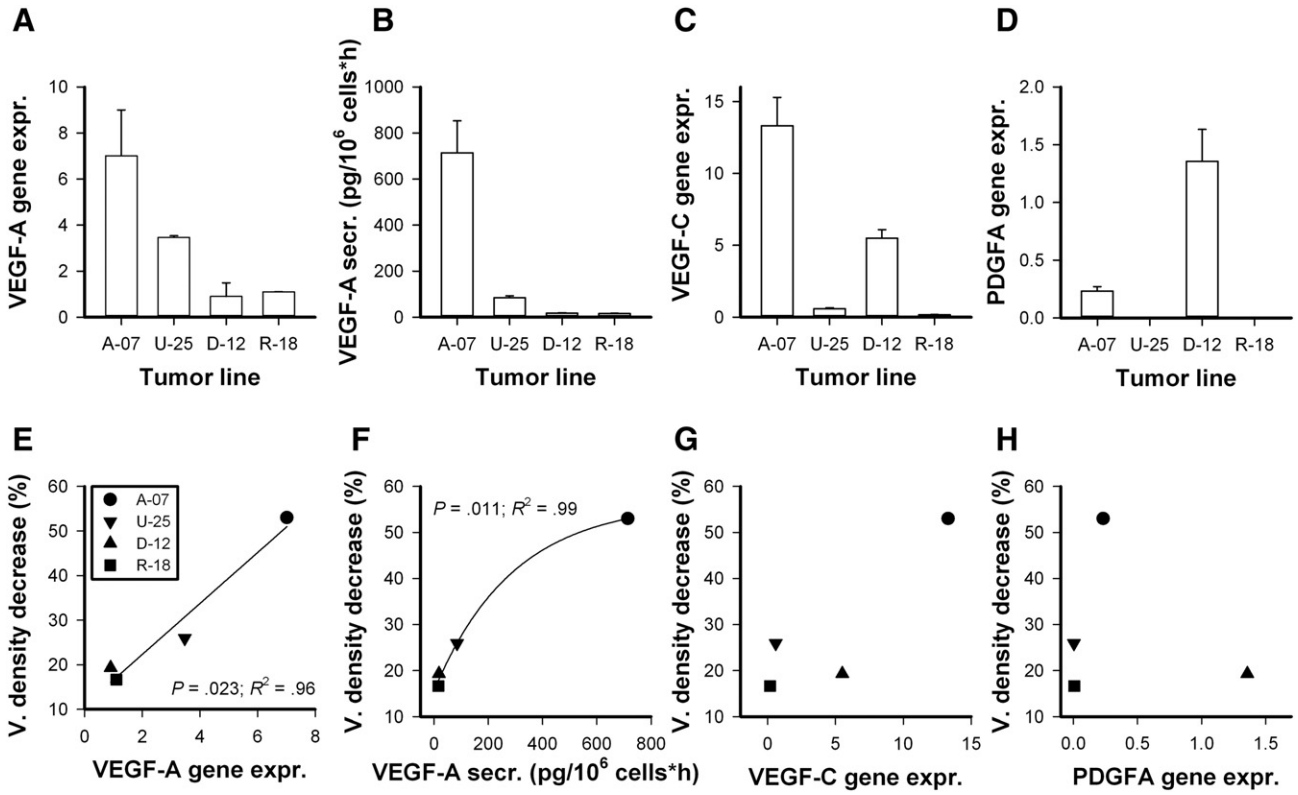

Figure 7. The effect of sunitinib treatment was associated with the gene expression and secretion rate of VEGF-A. (A–D) Normalized gene expression of VEGF-A (A), VEGF-C (C), and PDGFA (D), and protein secretion rate of VEGF-A (B) in the A-07, U-25, D-12, and R-18 cell line. Gene expression was measured with quantitative PCR, normalized to the mean expression of two housekeeping genes (GAPDH and ACTB), and multiplied with 1000. Protein secretion rates were measured with ELISA. Columns, mean of three (PCR) or five (ELISA) independent experiments; bars, SEM. (E–H) Vessel density decrease versus normalized gene expression of VEGF-A (E), VEGF-C (G), or PDGFA (H), and vessel density decrease versus protein secretion rate of VEGF-A (F). The vessel density decrease refers to the relative decrease in vessel density in sunitinib-treated tumors compared to untreated tumors and was calculated from Figure 3*A* ($[VD_{sun,\ day\ 4} - VD_{sun,\ day\ 0}]/VD_{sun,\ day\ 0} - [VD_{veh,\ day\ 4} - VD_{veh,\ day\ 0}]/VD_{veh,\ day\ 0}$). Lines, curves fitted to the data by regression analysis. R^2 and P values determined from regression analysis are indicated in the panels where statistical tests revealed significant correlations.

expression were not found ($P > .05$; Figure 7*G*). The sunitinib-induced decrease in vessel density was not correlated with PDGFA gene expression ($P > .05$; Figure 7*H*).

Discussion

The window chamber preparation is particularly well suited for evaluating treatment-induced effects on tumor vasculature because both the morphology and function of tumor vasculature can be studied repetitively by using intravital microscopy techniques [26,27]. In addition, the imaged tissue can be prepared and stained for hypoxia by immunohistochemistry, allowing detailed comparison of the tumor vasculature with the extent and localization of hypoxic regions.

Sunitinib treatment reduced vascular density and induced hypoxia in human melanoma xenografts. The treatment-induced increase in hypoxic fraction was probably a result of reduced oxygen supply caused by decreased vessel density. Thus, a significant correlation was found between hypoxic fraction and vessel density, and hypoxic regions colocalized with regions with low vascular density in sunitinib-treated tumors.

The magnitude of the sunitinib-induced effect differed among the four melanoma lines included in the study. The expression and secretion rate of VEGF-A also differed among the melanoma lines, and the treatment-induced decrease in vessel density was correlated with VEGF-A. VEGF-A induces angiogenesis by binding to VEGFR-2 on blood vessel endothelial cells [28], suggesting that inhibition of VEGFR-2 is important for the antiangiogenic effect observed in these melanoma lines. The melanoma lines also differed in the expression of VEGF-C and PDGFA. VEGF-C mainly induces lymphangiogenesis by binding to VEGFR-3 on lymph vessels, and the expression of PDGFA was not correlated to the sunitinib-induced decrease in vessel density. Taken together, these results suggest that the antiangiogenic effect observed in these melanoma lines was caused mainly by inhibition of VEGFR-2 rather than inhibition of VEGFR-3 and PDGFRs. This suggestion implies that melanoma patients with high VEGF-A–expressing tumors are more likely to respond to sunitinib treatment than patients with low VEGF-A–expressing tumors. Predictive biomarkers were searched for in a clinical phase II study investigating the effect of sunitinib treatment in unselected patients with advanced melanoma [29]. In this study, significant correlations between tumor response and baseline plasma levels of VEGF-A, VEGFR-1, or VEGFR-2 were not found. However, the number of samples included in the study were low, and the authors concluded that further study of these biomarkers remains of interest.

The current study suggests that some vessels were more affected by sunitinib treatment than others. Thus sunitinib-treated A-07 and D-12 tumors showed reduced fractions of small-diameter vessels, and sunitinib-treated tumors from all melanoma lines showed longer vessel segments. This observation is consistent with several studies reporting that antiangiogenic agents selectively remove immature blood vessels [12,13,30]. Changes in vascular morphology may affect the geometric resistance to blood flow. When laminar flow through a circular tube is assumed, the geometric resistance in a single vessel is proportional to the vessel length and inversely proportional to the vessel diameter to the fourth power [31]. We report that sunitinib treatment removed small-diameter vessels, inhibited growth-induced increases in the diameter of remaining vessels, and increased vessel segment lengths. Removal of small-diameter vessels is expected to reduce the geometric resistance, whereas inhibition of growth-induced increases in vessel diameters and increased vessel segment lengths are expected to increase the geometric resistance. Consistent with the opposing effects on geometric resistance, sunitinib treatment did not affect vascular function in these melanoma lines.

Sunitinib and other antiangiogenic treatments have improved vascular function in some experimental studies [4,30,32]. In these studies, the treatments have selectively removed immature vasculature and remodeled remaining vessels. Together, these have resulted in more efficient vessel networks, and as a consequence, increased blood flow velocities, increased blood perfusion, and increased oxygenation have been reported [4,30,32,33]. These effects have collectively been labeled vascular normalization and have been reported to occur within a short time period [34]. It has been argued that appropriate timing and low doses are required to observe vascular normalization because the beneficial effects on vascular function may be balanced by severe vascular regression after prolonged treatment or if the antiangiogenic treatment dose is too large [4,34]. Vascular function was assessed on day 2 and 4 in the present study. These time points correspond well to the time period where vascular normalization has been observed following treatment with bevacizumab (day 1-4), DC101 (day 2-5), and sunitinib (day 2-6) in other tumor models [4,30,32]. Moreover, both the same (40 mg/kg) and higher sunitinib doses (100 mg/kg) have been shown to improve vascular function in models of glioblastoma and renal cell carcinoma [32,35]. It is thus unlikely that improved vascular function could have been observed at other time points or by using smaller sunitinib doses in these melanoma models. Our study rather implies that, in some tumor models, sunitinib treatment does not improve vascular function. Similar observations have been made with bevacizumab and DC101 treatment [12,36].

Currently, clinical trials are evaluating whether antiangiogenic treatment in combination with immunotherapy or chemotherapy can improve survival for patients with malignant melanoma [9]. The rationale for combining antiangiogenic treatment with immunotherapy is that VEGF-A poses immunosuppressive effects in tumors [37]. Accordingly, it has been demonstrated that inhibition of VEGF-A/VEGFR-2 can increase the effect of immunotherapy in preclinical models [38]. However, it has also been reported that tumor hypoxia induces immunosuppression, suggesting that antiangiogenic treatment may reduce the effect of immunotherapy if the antiangiogenic treatment induces hypoxia [11,39]. Hypoxia also reduces the effect of ionizing radiation and some forms of chemotherapy, suggesting that neoadjuvant antiangiogenic treatment may reduce the effect of these treatment modalities if the antiangiogenic treatment induces hypoxia [10,14,40]. In contrast, it has been demonstrated that antiangiogenic treatments increase the effect of immunotherapy, chemotherapy, and ionizing radiation in tumor models where the antiangiogenic agents normalize the tumor vasculature and increase tumor oxygenation [3,30,41]. Antiangiogenic treatment may also affect the uptake of therapeutic drugs. Thus, impaired blood supply reduces the delivery of therapeutic drugs, whereas improved vascular function has been demonstrated to increase the uptake of chemotherapeutic drugs [3].

The current study demonstrates that sunitinib treatment reduces vessel density and induces hypoxia in four melanoma models with different angiogenic profile. This observation suggests that sunitinib treatment will induce hypoxia also in some patients with malignant melanoma and that neoadjuvant sunitinib treatment may decrease the effect of immunotherapy and conventional chemotherapy in such patients. However, our study does not exclude the possibility that sunitinib treatment may normalize tumor vasculature and increase oxygenation in some other melanoma patients and does not exclude the

possibility that treatment targeting other angiogenic pathways may increase oxygenation in tumors where sunitinib treatment induces hypoxia. Whether it is possible to predict if a specific antiangiogenic agent can increase oxygenation in individual tumors is not known. The effect of antiangiogenic treatment should thus be monitored closely if antiangiogenic treatment is considered as neoadjuvant therapy. We have previously demonstrated that dynamic contrast-enhanced and diffusion-weighted magnetic resonance imaging is sensitive to changes in the tumor microenvironment induced by sunitinib and bevacizumab treatment, suggesting that these noninvasive imaging techniques may be used to monitor the effect of antiangiogenic treatment [18,36].

The 4-day treatment period applied in the present study did not affect tumor growth. Treatment-induced reductions in vessel densities are expected to reduce tumor growth, but effects of antiangiogenic drugs on tumor size generally occur late [42]. In line with this, we have previously shown that short treatment periods with sunitinib (4 days) do not affect tumor growth, whereas prolonged treatment periods (8 days) reduce tumor growth rate in melanoma xenografts [19].

We have previously shown that hypoxia promotes invasive growth, and spontaneous lymph node and pulmonary metastasis in the melanoma models included in the current study [43–45]. One could thus speculate whether sunitinib-induced hypoxia may promote metastatic spread in these melanoma models. In accordance with this speculation, accelerated metastasis has been reported by others after sunitinib treatment in preclinical models [46–48]. However, sunitinib treatment may also inhibit metastatic growth by inhibiting angiogenesis at distant sites, and consequently, patients may benefit from sunitinib treatment after local tumor control has been achieved.

In summary, antiangiogenic agents have been reported to improve blood supply and oxygenation in some preclinical studies and to induce hypoxia in others. In the current study, sunitinib treatment reduced vessel density and induced hypoxia in human melanoma xenografts, and the magnitude of the effect was associated with the expression and secretion rate of VEGF-A. Our study suggests that sunitinib treatment will reduce vessel density and induce hypoxia also in some patients with malignant melanoma and that melanoma patients with high VEGF-A–expressing tumors are more likely to respond to sunitinib treatment than melanoma patients with low VEGF-A–expressing tumors.

Supplementary data to this article can be found online at http://dx.doi.org/10.1016/j.tranon.2016.12.007.

Funding

Financial support was received from the Norwegian Cancer Society and the South-Eastern Norway Regional Health Authority. The funding sources had no role in study design; in the collection, analysis, and interpretation of data; in the writing of the report; and in the decision to submit the article for publication.

Conflict of Interest

The authors confirm that there are no conflicts of interest.

References

[1] Folkman J (1990). What is the evidence that tumors are angiogenesis dependent? *J Natl Cancer Inst* **82**, 4–6.

[2] Carmeliet P and Jain RK (2000). Angiogenesis in cancer and other diseases. *Nature* **407**, 249–257.

[3] Dickson PV, Hamner JB, Sims TL, Fraga CH, Ng CY, Rajasekeran S, Hagedorn NL, McCarville MB, Stewart CF, and Davidoff AM (2007). Bevacizumab-induced transient remodeling of the vasculature in neuroblastoma xenografts results in improved delivery and efficacy of systemically administered chemotherapy. *Clin Cancer Res* **13**, 3942–3950.

[4] Winkler F, Kozin SV, Tong RT, Chae SS, Booth MF, Garkavtsev I, Xu L, Hicklin DJ, Fukumura D, and di Tomaso E, et al (2004). Kinetics of vascular normalization by VEGFR2 blockade governs brain tumor response to radiation: role of oxygenation, angiopoietin-1, and matrix metalloproteinases. *Cancer Cell* **6**, 553–563.

[5] Roskoski Jr R (2007). Sunitinib: a VEGF and PDGF receptor protein kinase and angiogenesis inhibitor. *Biochem Biophys Res Commun* **356**, 323–328.

[6] Jia Y, Liu M, Huang W, Wang Z, He Y, Wu J, Ren S, Ju Y, Geng R, and Li Z (2012). Recombinant human endostatin endostar inhibits tumor growth and metastasis in a mouse xenograft model of colon cancer. *Pathol Oncol Res* **18**, 315–323.

[7] Erhard H, Rietveld FJ, van Altena MC, Brocker EB, Ruiter DJ, and de Waal RM (1997). Transition of horizontal to vertical growth phase melanoma is accompanied by induction of vascular endothelial growth factor expression and angiogenesis. *Melanoma Res* **7**(Suppl. 2), S19–S26.

[8] Rofstad EK and Mathiesen B (2010). Metastasis in melanoma xenografts is associated with tumor microvascular density rather than extent of hypoxia. *Neoplasia* **12**, 889–898.

[9] Jour G, Ivan D, and Aung PP (2016). Angiogenesis in melanoma: an update with a focus on current targeted therapies. *J Clin Pathol* **69**, 472–483.

[10] Brown JM and Giaccia AJ (1998). The unique physiology of solid tumors: opportunities (and problems) for cancer therapy. *Cancer Res* **58**, 1408–1416.

[11] Hato T, Zhu AX, and Duda DG (2016). Rationally combining anti-VEGF therapy with checkpoint inhibitors in hepatocellular carcinoma. *Immunotherapy* **8**, 299–313.

[12] Franco M, Man S, Chen L, Emmenegger U, Shaked Y, Cheung AM, Brown AS, Hicklin DJ, Foster FS, and Kerbel RS (2006). Targeted anti-vascular endothelial growth factor receptor-2 therapy leads to short-term and long-term impairment of vascular function and increase in tumor hypoxia. *Cancer Res* **66**, 3639–3648.

[13] Fenton BM and Paoni SF (2007). The addition of AG-013736 to fractionated radiation improves tumor response without functionally normalizing the tumor vasculature. *Cancer Res* **67**, 9921–9928.

[14] Horsman MR and Siemann DW (2006). Pathophysiologic effects of vascular-targeting agents and the implications for combination with conventional therapies. *Cancer Res* **66**, 11520–11539.

[15] Demetri GD, van Oosterom AT, Garrett CR, Blackstein ME, Shah MH, Verweij J, McArthur G, Judson IR, Heinrich MC, and Morgan JA, et al (2006). Efficacy and safety of sunitinib in patients with advanced gastrointestinal stromal tumour after failure of imatinib: a randomised controlled trial. *Lancet* **368**, 1329–1338.

[16] Motzer RJ, Hutson TE, Tomczak P, Michaelson MD, Bukowski RM, Oudard S, Negrier S, Szczylik C, Pili R, and Bjarnason GA, et al (2009). Overall survival and updated results for sunitinib compared with interferon alfa in patients with metastatic renal cell carcinoma. *J Clin Oncol* **27**, 3584–3590.

[17] Raymond E, Hammel P, Dreyer C, Maatescu C, Hentic O, Ruszniewski P, and Faivre S (2012). Sunitinib in pancreatic neuroendocrine tumors. *Target Oncol* **7**, 117–125.

[18] Gaustad JV, Pozdniakova V, Hompland T, Simonsen TG, and Rofstad EK (2013). Magnetic resonance imaging identifies early effects of sunitinib treatment in human melanoma xenografts. *J Exp Clin Cancer Res* **32**, 93.

[19] Gaustad JV, Simonsen TG, Leinaas MN, and Rofstad EK (2012). Sunitinib treatment does not improve blood supply but induces hypoxia in human melanoma xenografts. *BMC Cancer* **12**, 388.

[20] Rofstad EK (1994). Orthotopic human melanoma xenograft model systems for studies of tumour angiogenesis, pathophysiology, treatment sensitivity and metastatic pattern. *Br J Cancer* **70**, 804–812.

[21] Gaustad JV, Brurberg KG, Simonsen TG, Mollatt CS, and Rofstad EK (2008). Tumor vascularity assessed by magnetic resonance imaging and intravital microscopy imaging. *Neoplasia* **10**, 354–362.

[22] Øye KS, Gulati G, Graff BA, Gaustad JV, Brurberg KG, and Rofstad EK (2008). A novel method for mapping the heterogeneity in blood supply to normal and malignant tissues in the mouse dorsal window chamber. *Microvasc Res* **75**, 179–187.

[23] Rofstad EK and Måseide K (1999). Radiobiological and immunohistochemical assessment of hypoxia in human melanoma xenografts: acute and chronic hypoxia in individual tumours. *Int J Radiat Biol* **75**, 1377–1393.

[24] Simonsen TG, Gaustad JV, Leinaas MN, and Rofstad EK (2012). High interstitial fluid pressure is associated with tumor-line specific vascular abnormalities in human melanoma xenografts. *PLoSOne* **7**, e40006.

[25] Rofstad EK and Halsør EF (2000). Vascular endothelial growth factor, interleukin 8, platelet-derived endothelial cell growth factor, and basic fibroblast

growth factor promote angiogenesis and metastasis in human melanoma xenografts. *Cancer Res* **60**, 4932–4938.
[26] Jain RK, Munn LL, and Fukumura D (2002). Dissecting tumour pathophysiology using intravital microscopy. *Nat Rev Cancer* **2**, 266–276.
[27] Tozer GM, Ameer-Beg SM, Baker J, Barber PR, Hill SA, Hodgkiss RJ, Locke R, Prise VE, Wilson I, and Vojnovic B (2005). Intravital imaging of tumour vascular networks using multi-photon fluorescence microscopy. *Adv Drug Deliv Rev* **57**, 135–152.
[28] Lohela M, Bry M, Tammela T, and Alitalo K (2009). VEGFs and receptors involved in angiogenesis versus lymphangiogenesis. *Curr Opin Cell Biol* **21**, 154–165.
[29] Decoster L, Vande Broek I, Neyns B, Majois F, Baurain JF, Rottey S, Rorive A, Anckaert E, De Mey J, and De Brakeleer S, et al (2015). Biomarker analysis in a phase II study of sunitinib in patients with advanced melanoma. *Anticancer Res* **35**, 6893–6899.
[30] Dings RP, Loren M, Heun H, McNiel E, Griffioen AW, Mayo KH, and Griffin RJ (2007). Scheduling of radiation with angiogenesis inhibitors anginex and Avastin improves therapeutic outcome via vessel normalization. *Clin Cancer Res* **13**, 3395–3402.
[31] Jain RK (1988). Determinants of tumor blood flow: a review. *Cancer Res* **48**, 2641–2658.
[32] Czabanka M, Vinci M, Heppner F, Ullrich A, and Vajkoczy P (2009). Effects of sunitinib on tumor hemodynamics and delivery of chemotherapy. *Int J Cancer* **124**, 1293–1300.
[33] Cao Y, Sonveaux P, Liu S, Zhao Y, Mi J, Clary BM, Li CY, Kontos CD, and Dewhirst MW (2007). Systemic overexpression of angiopoietin-2 promotes tumor microvessel regression and inhibits angiogenesis and tumor growth. *Cancer Res* **67**, 3835–3844.
[34] Jain RK (2005). Normalization of tumor vasculature: an emerging concept in antiangiogenic therapy. *Science* **307**, 58–62.
[35] Lee JA, Biel NM, Kozikowski RT, Siemann DW, and Sorg BS (2014). In vivo spectral and fluorescence microscopy comparison of microvascular function after treatment with OXi4503, sunitinib and their combination in Caki-2 tumors. *Biomed Opt Express* **5**, 1965–1979.
[36] Gaustad JV, Simonsen TG, Smistad R, Wegner CS, Andersen LM, and Rofstad EK (2015). Early effects of low dose bevacizumab treatment assessed by magnetic resonance imaging. *BMC Cancer* **15**, 900.
[37] Ott PA, Hodi FS, and Buchbinder EI (2015). Inhibition of immune checkpoints and vascular endothelial growth factor as combination therapy for metastatic melanoma: an overview of rationale, preclinical evidence, and initial clinical data. *Front Oncol* **5**, 202.
[38] Manning EA, Ullman JG, Leatherman JM, Asquith JM, Hansen TR, Armstrong TD, Hicklin DJ, Jaffee EM, and Emens LA (2007). A vascular endothelial growth factor receptor-2 inhibitor enhances antitumor immunity through an immune-based mechanism. *Clin Cancer Res* **13**, 3951–3959.
[39] Facciabene A, Peng X, Hagemann IS, Balint K, Barchetti A, Wang LP, Gimotty PA, Gilks CB, Lal P, and Zhang L, et al (2011). Tumour hypoxia promotes tolerance and angiogenesis via CCL28 and T(reg) cells. *Nature* **475**, 226–230.
[40] Stone HB, Bernhard EJ, Coleman CN, Deye J, Capala J, Mitchell JB, and Brown JM (2016). Preclinical data on efficacy of 10 drug-radiation combinations: evaluations, concerns, and recommendations. *Transl Oncol* **9**, 46–56.
[41] Huang Y, Yuan J, Righi E, Kamoun WS, Ancukiewicz M, Nezivar J, Santosuosso M, Martin JD, Martin MR, and Vianello F, et al (2012). Vascular normalizing doses of antiangiogenic treatment reprogram the immunosuppressive tumor microenvironment and enhance immunotherapy. *Proc Natl Acad Sci U S A* **109**, 17561–17566.
[42] Morgan B, Horsfield MA, and Steward WP (2004). The role of imaging in the clinical development of antiangiogenic agents. *Hematol Oncol Clin North Am* **18**, 1183–1206.
[43] Rofstad EK, Rasmussen H, Galappathi K, Mathiesen B, Nilsen K, and Graff BA (2002). Hypoxia promotes lymph node metastasis in human melanoma xenografts by up-regulating the urokinase-type plasminogen activator receptor. *Cancer Res* **62**, 1847–1853.
[44] Rofstad EK, Gaustad JV, Egeland TA, Mathiesen B, and Galappathi K (2010). Tumors exposed to acute cyclic hypoxic stress show enhanced angiogenesis, perfusion and metastatic dissemination. *Int J Cancer* **127**, 1535–1546.
[45] Rofstad EK and Halsør EF (2002). Hypoxia-associated spontaneous pulmonary metastasis in human melanoma xenografts: involvement of microvascular hot spots induced in hypoxic foci by interleukin 8. *Br J Cancer* **86**, 301–308.
[46] Ebos JM, Lee CR, Cruz-Munoz W, Bjarnason GA, Christensen JG, and Kerbel RS (2009). Accelerated metastasis after short-term treatment with a potent inhibitor of tumor angiogenesis. *Cancer Cell* **15**, 232–239.
[47] Paez-Ribes M, Allen E, Hudock J, Takeda T, Okuyama H, Vinals F, Inoue M, Bergers G, Hanahan D, and Casanovas O (2009). Antiangiogenic therapy elicits malignant progression of tumors to increased local invasion and distant metastasis. *Cancer Cell* **15**, 220–231.
[48] Yin T, He SS, Ye TH, Shen GB, Wan Y, and Wang YS (2014). Antiangiogenic therapy using sunitinib combined with rapamycin retards tumor growth but promotes metastasis. *Transl Oncol* **7**, 221–229.